Fermi National Accelerator Laboratory

FERMILAB-Pub-92-323-A

ON USING A NEUTRINO MAGNETIC MOMENT TO ATTACK THE SOLAR NEUTRINO PROBLEM *

X. Shi,[1] D.N. Schramm,[1,2,3] R. Rosner,[2] and D.S. Dearborn[4]
[1]Department of Physics
and
[2]Department of Astronomy and Astrophysics
University of Chicago, 5640 S. Ellis Ave., Chicago IL 60637
[3]NASA/Fermilab Astrophysics Center
Box 500, Batavia, IL 60510
[4]Lawrence Livermore National Laboratory
Livermore, CA 94550

Abstract

The matter-enhanced spin-flavor precession of the solar neutrinos as a possible solution to the solar neutrino problem is revisited. It is argued that in order to explain the possible anti-correlation between the neutrino flux and the solar activity in the Homestake experiment, the neutrino magnetic resonance must occur with substantial amplitude in the convective zone. The maximal magnetic field inside the solar convective zone is discussed in detail. Combining these constraints with the astrophysical constraints on the neutrino magnetic moment, and data from the ^{37}Cl Homestake experiment, and numerical models of the Sun, it is shown that, by itself, the spin-flavor precession of solar neutrinos cannot simultaneously explain the observed neutrino flux and possible anti-correlations of the Homestake experiment. An appendix is devoted to the statistical questions of possible anti-correlations.

* Submitted to *Comments on Nucl. and Part. Physics*

Introduction

Twenty years of solar neutrino observations in the Homestake chlorine capture experiment indicate a substantial solar neutrino deficit: the chlorine capture experiment yields 2.1±0.3 SNU,[1] compared to 7.9 SNU of Standard Solar Model (SSM) of Bahcall *et al.*,[2] or 6.4 SNU for the Turck-Chièze model[3]. A deficit is confirmed by the Kamiokande II electron scattering experiment, which yields a flux $0.46 \pm 0.05(stat) \pm 0.06(syst)$ times the prediction of the SSM of Bahcall *et al.*,[4] and two gallium capture experiments, SAGE and GALLEX. SAGE reported recently a flux of $58^{+17}_{-24}(stat) \pm 14(syst)$ SNU,[5] with respect to 132 SNU of SSM.[2] GALLEX reported a capture rate of $83 \pm 19(stat) \pm 8(syst)$ SNU.[6] A purely astrophysical solution would require a major unanticipated systematic error in the ^{37}Cl experiment. New neutrino physics has been suggested to solve the puzzle.[7] Among these new physics solutions, the Mikheyev-Smirnov-Wolfenstein (MSW) matter mixing solution is particularly robust and elegant.[8] Under the MSW matter mixing scheme, solar neutrinos (ν_e) mix with ν_μ or ν_τ (or both). On their way out of the sun, ν_e encounter a resonance inside the sun and flip their flavor.

Another plausible neutrino physics solution, motivated by the observation of the Homestake experiment that an anti-correlation might exist between the solar neutrino flux and the sunspot activity,[9] was suggested by Okun, Voloshin and Vysotsky (OVV).[10] In this scenario, the neutrino possesses a magnetic moment. The spin precession of the solar neutrinos in the solar magnetic field converts ν_{e_L} into sterile ν_{l_R} ($l = e, \mu$ or τ) and creates the flux depletion in the chlorine experiment. During a sunspot active year, the magnetic field is strong in the solar convective zone, and more ν_{e_L} are depleted, which yields a smaller observed flux. During a sunspot quiet year, vice versa, the observed flux is higher. If this anti-correlation in the chlorine experiment is a real physical effect, the neutrino magnetic moment solution seems the most plausible, since otherwise it is hard to correlate the neutrino produced at the central core of the Sun with the activity at the solar surface. However, the anti-correlation is still very controversial. Its statistical significance has been questioned and it has not been confirmed by the other long-running experiment, the Kamiokande II experiment.[4] Some have argued that the variations in the ^{37}Cl experiment indicate a problem with the experiment itself rather than a real solar neutrino effect.[11] (In the appendix to this paper we discuss the statistics of the claimed anti-correlation in the Homestake experiment in more detail.) Despite the controversy, we will re-examine the neutrino magnetic moment solution, and explore the magnitude of any anti-correlation for extreme upper limits on the neutrino magnetic moment and the solar magnetic field. We will argue that the average solar magnetic field at the bottom of the convective zone is reliably constrained to $B \lesssim 10^4$ Gauss. Since only fields in or near the convective zone vary with the solar activity, this is the critical field strength. We will show that with this field constraint and the astrophysical constraint on the neutrino magnetic moment, $\mu \leq 3(2) \times 10^{-12}\mu_B$ for the Majorana and diagonal Dirac (transitional Dirac) neutrino magnetic moments, the OVV scenario fails to yield an anti-correlation between the neutrino flux and the solar activity that is large enough to be observable in the chlorine experiment. If there is any sort of statistically significant anti-correlation with the sunspot numbers shown in the chlorine experiment, then our study might imply a possible systematic problem with the chlorine experiment itself.

The Neutrino Magnetic Moment

In the Standard Model, the neutrino acquires a magnetic moment proportional to its mass from radiative corrections,[12]

$$\mu \approx 3 \times 10^{-19}\mu_B(\frac{m}{1\text{eV}}), \tag{1}$$

where μ_B is the Bohr magneton, and m is the neutrino mass. The magnitude of this moment is too small to be of any interest in the solar neutrino problem for an electron-neutrino mass less than 1 MeV. New neutrino physics can be introduced to give a neutrino magnetic moment as large as $10^{-10}\mu_B$, which is roughly the scale needed to play a role in the solar neutrino problem.[13] Some of these models can yield not only the diagonal magnetic moments, which convert the left-handed neutrino into the right-handed neutrino of the same flavor (apply to Dirac neutrinos only), but also off-diagonal (transition) moments, which convert the left-handed neutrino into the right-handed neutrino of another flavor (apply to both Dirac neutrinos and Majorana neutrinos).

There have been various bounds on the neutrino magnetic moment. Antineutrino electron scattering experiments search for the cross section in excess of the standard weak theory and set a bound on the magnetic moment[14]

$$|\mu_{\nu_e}| \leq 4 \times 10^{-10}\mu_B. \tag{2}$$

More stringent bounds come from astrophysical and cosmological arguments.

If neutrinos have magnetic moments, the plasmon decay $\gamma^* \to \nu\bar{\nu}$ will speed up the stellar cooling process, especially the cooling of white dwarfs, where the plasma density is very high. Observations on the cooling of young white dwarfs then set a bound[15]

$$(\sum_{i,j} |\mu_{ij}|^2)^{1/2} \leq 7 \times 10^{-11}\mu_B, \tag{3}$$

where i, j denote neutrino species.

The magnetic moment for Dirac neutrinos can be translated into extra degrees of freedom in neutrino species during the Big Bang Nucleosynthesis. As a result, the observed primordial helium abundance yields a constraint[16]

$$|\mu_\nu| \leq 1.5 \times 10^{-11} \mu_B \tag{4}$$

for Dirac neutrinos.

The neutrino observation from SN1987a could also impose bounds on the Dirac neutrino magnetic moment. The bulk of the energy (more than 90%) released by supernova events is carried out by neutrinos. If neutrinos have a finite magnetic moment, conversions of left-handed neutrinos to right-handed neutrinos will happen when neutrinos scatter off nucleons and electrons. As a result the right-handed neutrinos will stream out of the protoneutron star nearly freely and provide a very efficient way to cool the neutron star. The signals of SN1987a neutrinos observed by the Kamiokande and IMB experiments indicate a cooling time of several seconds,[17] which agrees with standard stellar collapse theory, and yields a bound on the neutrino magnetic moment[18]

$$|\mu_{\nu_e}| \leq 0.1\text{--}1 \times 10^{-12} \mu_B. \tag{5}$$

It has also been argued that a finite neutrino magnetic moment will generate a "collapse burst" of right-handed neutrino during the core collapse. These high energy (200–300 MeV) right-handed neutrinos will flip their spins in the galactic magnetic field and lead to many more supernova neutrino events than observed. Such consideration of the emission of the right-handed neutrinos during the core collapse gives[19]

$$|\mu_{\nu_e}| \leq 1.5 \times 10^{-12} \mu_B. \tag{6}$$

Also consideration that the emission of the right-handed neutrinos during the core collapse will affect the energy of the shock wave after the bounce yields[19]

$$|\mu_{\nu_e}| \leq 6 \times 10^{-12} \mu_B. \tag{6'}$$

However, bounds from the supernova have been questioned. Voloshin[20] argued that if strong magnetic fields exist in the supernova, the right-handed neutrino will be resonantly converted back to left-handed neutrinos before they can stream out of the core. A field as strong as 10^{12} Gauss will allow a neutrino magnetic moment of $10^{-11}\mu_B$ without conflicting with the considerations above.[20]

Another astrophysical constraint comes from consideration of the luminosity before and after stellar helium flash.[21] Before helium burning, the red giants are fueled by a thin hydrogen-burning shell outside the helium core. When more and more helium is deposited into the core, the helium gets ignited and begins to burn while the core is still supported by electron degeneracy pressure. The sudden energy release of helium creates a momentary nuclear runaway ("helium flash") that dramatically overshoots the degeneracy pressure and leads to a core expansion until a new equilibrium is reached. Such expansion reduces the gravitational potential of the hydrogen-burning shell, and leads to a drop in the luminosity which cannot be compensated by the helium burning. A finite neutrino magnetic moment will cool the helium core more efficiently (due to the same plasmon decay mechanism) before the flash and delay its occurance. Such delay will lead to a larger mass deposited in the helium core and a different luminosity drop before and after the helium flash. Observation of such variation, compared with the stellar evolution calculations then yields[21]

$$\mu_\nu \leq 3 \times 10^{-12} \mu_B, \tag{7}$$

where $\mu_\nu = (\sum_{i,j} |\mu_{ij}|^2)^{1/2}$ for Dirac neutrinos and $\mu_\nu = (\sum_{i,j} |\mu_{ij}|^2)^{1/2}/2$ for Majorana neutrinos. This translates into a bound on the transitional Majorana neutrino magnetic moment

$$\mu_{ij} \leq 3 \times 10^{-12} \mu_B, \tag{7-1}$$

and a bound on the transitional Dirac neutrino magnetic moment

$$\mu_{ij} \leq 2 \times 10^{-12} \mu_B, \tag{7-2}$$

when the diagonal components are zero, or

$$\mu_{ii} \leq 3 \times 10^{-12} \mu_B, \tag{7-3}$$

when the transitional components and other diagonal components are zero. Since these arguments appear well substantiated and rather conservative, Eq. (7) is the bound we will adopt in the following discussion.

The Solar Magnetic Field

The configuration and the strength of the solar interior magnetic field are not quite clear. One can only make observations of the magnetic activity at the surface of the Sun and infer the field inside. Observations have shown that the magnetic activity at solar surface is very complex and dynamical.[22] The most distinct feature is the ~11-year cycle of the number of sunspots, where the larger magnetic flux bundles emerge and cool the surface temperature to ~ 2/3 of that of the surrounding area. During the active period of the cycle, magnetic flux erupts from the solar interior and congregates to form active regions and active region complexes, with local field strengths ranging from ~1500 to ~3000 Gauss, between an approximate latitude range of ±40°. The emerging magnetic fields also lead to enhanced coronal and chromospheric activity, associated with plasma heating to temperatures in excess of 10^7 K in solar flares. Larger sunpots and active regions can persist for months; as these disappear, new magnetic eruptions continue to occur at lower latitudes. Eventually, on a time scale of ~5–6 years, these activities fade away, as the Sun reaches the quiet period of its activity cycle. At the end of this cycle, new magnetic eruptions occur at middle latitudes of approximatly $\pm 40°$, and a new active period ensues. Observations suggest that the main components of the fields erupting at the solar surface are derived from toroidal interior fields, a conclusion which follows from the regularity of the polarity and orientation of emerging, leading and following (in latitude) sunspots and sunspot groups.

The standard solar model has had a great success in predicting the Sun's thermal structure and evolution.[7] In contrast, our understanding of the Sun's activity cycle is very primitive. We do not have a generally accepted theory of the solar magnetic dynamo;[23,24] we do not understand why the Sun's surface fields are so highly intermittent; and we have no generally accepted model which integrates the Sun's magnetic activity history into its thermal history and nuclear evolution.

Nevertheless, it has been possible to construct very general arguments which, for example, bound the strength of interior magnetic fields. In particular, a magnetic field of order 10^9 Gauss in the solar core was proposed to reduce the core temperature and thereby reduce the solar neutrino production.[7] But it was shown by Parker that a field in excess of 0.5×10^8 Gauss in the central core would be lost from the Sun during its history as a consequence of its buoyancy.[25] Magnetic fields less than 10^9 Gauss in the solar core or less than 10^7 Gauss in the convective zone will hardly affect the thermal structure and the nuclear reaction process of the Sun, which are well described by the standard solar model. Nor does it affect the steady state solar neutrino flux appreciably.

More stringent bounds on the magnetic field strength in the convective part of the Sun can be imposed as follows. First, consider the fact that $\sim 10^{24\pm1}$ Gauss$\cdot$cm^2 of magnetic flux emerges from the solar interior during one activity cycle.[26] If this flux is stored within the entire convection zone between approximate latitudes $\pm 40°$, then the mean strength of the stored interior field is $\sim 10^3$ G. If instead the flux is stored in a boundary layer at the base of the convective zone, then the corresponding mean field strength is $\sim 1.5\times10^4(10^4\mathrm{km}/d)$ G, where d is the thickness of the boundary layer, and is likely to be at least a few tenths of the pressure scale height at the base of the convective zone.[27]

A second limit is based on the nonlinear effects which ultimately must limit the growth of magnetic fields created by the dynamo process.[28] In the simple mixing length picture, a naive limit on the field can be estimated by calculating the field tension needed to prevent a bubble of fluid from sinking into a magnetically stratified region (thus limiting further flux amplification). When a fluid element sinks in the bottom of the convective zone, it has an energy excess $c_\rho \rho \Delta T$ with respect to the surrounding fluids, where $\Delta T = -\int_{r_1}^{r_2} (\nabla - \nabla_{adia}) T \cdot \mathbf{dr}$ ($\nabla_{adia} T$ is the temperature gradient assuming adiabatic mixing in the convective zone). In the nonlocal mixing length theory, $\nabla - \nabla_{adia}$ is typically of order $10^{-7} \nabla_{adia}$.[29] By equating the magnetic tension to the energy excess of a sinking element,

$$B^2/4\pi \sim c_\rho \rho \Delta T, \tag{8}$$

and taking $C_\rho = 4 \times 10^8 \text{ergs} \cdot \text{g}^{-1} \cdot \text{K}^{-1}$, $\rho = 0.26 \text{g/cm}^3$, and $\Delta T = 0.2\text{K}$,[29] Schmitt and Rosner obtained a limiting field strength of $\sim$ 10000 Gauss.[28] Large-scale fields (other than field ropes) in excess of 10000 Gauss will certainly exclude the turbulent motions and force the convective zone to recede upwards, hence suppressing further growth of the field. Apparently, this limit depends on the calculation of ΔT. If we simply multiply $10^{-7} \nabla_{adia} T$ by $\sim 10^4$ km, we get $\Delta T \sim 10^{-2}$ to 10^{-1} K, which is smaller than the value adopted above. Therefore the average field limit obtained above is very reasonable. We also note that our limit is very conservative because detailed calculations have shown field amplification to saturate at far lower strengths than adduced here.[30]

It should be noted that the 10^4 Gauss limit we obtained from Eq. (8) is the limit on the average fields in the convective zone, i.e., large-scale fields that have ranges comparable to the mixing length. Small-scale field ropes as strong as 10^5 Gauss in a scale of $\sim 10^3$ km is possible at the bottom of the convective zone. But we will show later that such field ropes play little role in the depletion of left-handed neutrinos due to their short ranges.

Parker obtained a limit on the magnetic field in the convective zone by considering the ^{7}Li abundance in the solar convective zone.[31] The observed ratio of ^{7}Li abundance to H abundance at the solar surface is 10^{-12},[32] which is 10^2 times lower than the cosmic abundance, 10^{-10}.[33] On the one hand, since calculations show that ^{7}Li was depleted by about a half during its pre-main-sequence stage, the observation indicates that it is depleted by a factor of 50 through nuclear reactions in the Sun after the Sun entered the main sequence. On the other hand, since ^{7}Li is so fragile (^{7}Li begins to burn at a temperature $T = 2.5 \times 10^6$ K), its existance in the Sun indicates that it hasn't been consumed completely during the main-sequence stage, which is about 4.5×10^9 years long. The bottom of the solar convective zone, located at 2×10^5 km deep, has a temperature $T = 2.2 \times 10^6$ K. At another 3×10^4 km deeper, the temperature reaches $T = 2.5 \times 10^6$ K. Parker showed that a field as strong as 4×10^5 Gauss and extending 3×10^4 km at the bottom of the convective zone would force the convetive zone to extend deep enough to sufficiently destroy the ^{7}Li abundance in the Sun, while not destroying it completely during 4.5×10^9 years.

Whether or not there exists a strong field in the solar radiative interior is still an open question. If it exists, it is rather stable, at least on the 11-year time scale, because of the stable structure of the radiative interior. A primordial magnetic field of 10^7 Gauss is possible but it may not persist during the Hayashi phase when the Sun was entirely convective.[34] Even though this field could be strong enough to deplete the solar neutrino flux to the observed value without intruding the bound on the neutrino magnetic moment, it couldn't yield a flux with an 11-year variation. Therefore, in order to yield the observed flux and the variation with the neutrino magnetic moment scenario, we have to rely on the large-scale magnetic field in the convective zone.

Discussion and Numerical Results

Only the magnetic field components that are perpendicular to the momentum of neutrinos can flip their spins.[10] In the solar convective zone, the toroidal fields are the main component of the magnet fields. Therefore the field limits obtained in the previous section are also the limits on the fields that are responsible for the depletion of solar neutrinos. As we will see later, the quantity that comes into play in the solar neutrino problem is $|\mu B|$, instead of μ and B individually. Eq. (7) and the bound on the (large-scale) convective magnetic field $B \lesssim 10000$ Gauss gives us

$$|\mu B| \lesssim 3(2) \times 10^{-12}\mu_B \cdot 10^4\text{Gauss} = 1.7(1.2) \times 10^{-16}\text{eV} \tag{9}$$

for Majorana and diagonal Dirac (transitional Dirac) neutrino moments. This is the bound on $|\mu B|$ at the bottom of the convective zone. Above the bottom of the convective zone, the field is weaker. At the surface, where $B \lesssim 10^3$ Gauss during the solar active period, the bound should be an order of magnitude smaller than Eq. (9). Since the distribution of the field in the convective zone is complicated and largely unknown, we assume a uniform field for simplicity, an assumption which will also give us an upper limit to the real case. In the spin-flavor resonance solution we will discuss later, the resonances occur at the lower part of the convective zone for the mixing parameters we will discuss. Therefore the field at the surface doesn't play an essential role in the problem and a uniform field configuration suffices in our discussion.

To be even more conservative, we explore the situation with a bound of

$$|\mu B| \leq 1(0.7) \times 10^{-7}\mu_B \cdot \text{Gauss} = 6(4) \times 10^{-16}\text{eV} \tag{10}$$

in our calculation, corresponding to a neutrino magnetic moment of $1\ (0.7)\times 10^{-11}\mu_B$ and a field of 10^4 Gauss, or a magnetic moment of $3\ (2)\times 10^{-12}\mu_B$ and a field of $3.4\ \times 10^4$ Gauss, for the Majorana and diagonal Dirac (transitional Dirac) neutrino magnetic moments. From our previous discussion these are extremely generous values.

Eq. 7 and the bound on the magnetic field from ^{7}Li gives a bound

$$|\mu B| \leq 7(5) \times 10^{-15}\text{eV} \tag{11}$$

for Majorana and diagonal Dirac (transitional Dirac) neutrino moments.

The Homestake experiment has a capture rate 2.1 ± 0.3 SNU averaging over all running years, which implies that the capture rate should be smaller than 2.7 SNU in solar active years, at 95% C. L.. The claim of an anti-correlation in the chlorine experiment requires the ratio of the capture rates in active years to the rates in quiet years to be considerably smaller than 1. Since the 1σ error of the chlorine experiment is about 15%, it is fair to require a ratio less than 0.7 to be observable in the experiment. For simplicity and to optimize the effect, we assume that the solar magnetic field in the convective zone is fully turned on in active years, and is zero in quiet years. In order for the spin flip mechanism to work, it is necessary to find a neutrino mixing parameter space that satisfies

$$R = \phi_B/\phi_0 < 0.7, \quad \text{and} \quad \phi_B < 2.7 \text{ SNU} \tag{12}$$

where ϕ_B is the capture rate when the solar convective field is on, and ϕ_0 is the capture rate when no field is present.

If ν_e only has a diagonal magnetic moment μ, the Schrödinger equation evolving ν_e is[35]

$$i\frac{d}{dt}\begin{pmatrix}\nu_{e_L}\\ \nu_{e_R}\end{pmatrix} = \begin{pmatrix}a_e(t) & \mu B(t)\\ \mu B(t) & 0\end{pmatrix}\begin{pmatrix}\nu_{e_L}\\ \nu_{e_R}\end{pmatrix} \tag{13}$$

where a_e is the induced electron neutrino mass in matter, which is given by

$$a_e(t) = \frac{G_F}{\sqrt{2}}(2N_e - N_n), \tag{14}$$

where N_e and N_n are electron and neutron densities respectively. For $R > 0.2R_\odot$, we have

$$N_n \approx N_e/6. \tag{15}$$

Equation (13) resembles the equation of neutrino vacuum oscillation except a_e changes with time. In analogy to vacuum mixing, for two neutrino state mixing, the solar neutrino flux is at most depleted by half even assuming maximal mixing, which requires $\mu B \gg a_e$. But for the most of the Sun ($R < 0.9R_\odot$), N_e is larger than $1 \times 10^{22}\text{cm}^{-3}$,[36] which implies that

$$a_e > 1.2 \times 10^{-15}\text{eV} > \mu B. \tag{16}$$

For the remaining $0.1R_\odot$, the distance is much less than the neutrino oscillation length l_{osc}, where

$$l_{osc} \sim \frac{\pi\hbar c}{|\mu B|} > 1 \times 10^9\text{m} \gg 0.1R_\odot. \tag{17}$$

As a result no appreciable oscillations can occur. (In the presence of 10^5 Gauss field ropes in the convective zone, following the same calculation, the oscillation length is about 10^5

km, which is much larger than the typical size of the ropes, $\sim 10^3$ km. As a result these small-scale fields don't help depleting solar neutrinos appreciably either.) Therefore the simple diagonal magnetic moment scenario cannot result in the observed neutrino flux depletion and observable neutrino flux variations.

To acquire a larger flux depletion, we might appeal to a mixing between different flavors via transitional magnetic moments and also include the MSW effect. This is the so-called resonant spin-flavor precession.[35]

The general form of the Schrödinger equation for two neutrino species (for illustrative purpose, we assume ν_e and ν_μ mixing) with magnetic moments in matter is:

$$i\frac{d}{dt}\begin{pmatrix} \nu_{e_L} \\ \nu_{\mu_L} \\ \nu_{e_R} \\ \nu_{\mu_R} \end{pmatrix} = H \begin{pmatrix} \nu_{e_L} \\ \nu_{\mu_L} \\ \nu_{e_R} \\ \nu_{\mu_R} \end{pmatrix} \tag{18}$$

H is the Hamiltonian for the system:

$$H_{Dirac} = \begin{pmatrix} \frac{\Delta m^2}{2E} sin^2\theta + a_e & \frac{\Delta m^2}{4E} sin2\theta & \mu_{ee}^* B & \mu_{\mu e}^* B \\ \frac{\Delta m^2}{4E} sin2\theta & \frac{\Delta m^2}{2E} cos^2\theta + a_\mu & \mu_{e\mu}^* B & \mu_{\mu\mu}^* B \\ \mu_{ee} B & \mu_{e\mu} B & \frac{\Delta m^2}{2E} sin^2\theta & \frac{\Delta m^2}{4E} sin2\theta \\ \mu_{\mu e} B & \mu_{\mu\mu} B & \frac{\Delta m^2}{4E} sin2\theta & \frac{\Delta m^2}{2E} cos^2\theta \end{pmatrix}. \tag{19}$$

and

$$H_{Majorana} = \begin{pmatrix} \frac{\Delta m^2}{2E} sin^2\theta + a_e & \frac{\Delta m^2}{4E} sin2\theta & 0 & \mu_{\mu e}^* B \\ \frac{\Delta m^2}{4E} sin2\theta & \frac{\Delta m^2}{2E} cos^2\theta + a_\mu & -\mu_{e\mu}^* B & 0 \\ 0 & -\mu_{e\mu} B & \frac{\Delta m^2}{2E} sin^2\theta - a_e & \frac{\Delta m^2}{4E} sin2\theta \\ \mu_{\mu e} B & 0 & \frac{\Delta m^2}{4E} sin2\theta & \frac{\Delta m^2}{2E} cos^2\theta - a_\mu \end{pmatrix}. \tag{19'}$$

where

$$a_e = \frac{G_F}{\sqrt{2}}(2N_e - N_n), \quad a_\mu = -\frac{G_F}{\sqrt{2}} N_n. \tag{20}$$

Given Eq. (19) and Eq. (19′), two resonances could possibly occur while the solar neutrino ν_{e_L} propagates though the Sun.[35] The $\nu_{e_L} \to \nu_{\mu_R}$ spin resonance occur at a higher density where

$$\frac{\Delta m^2}{2E} cos2\theta = \frac{G_F}{\sqrt{2}}(2N_e - N_n) \approx \frac{11}{12}\sqrt{2} G_F N_e \quad \text{for Dirac neutrinos,}$$

$$\frac{\Delta m^2}{2E} cos2\theta = \frac{G_F}{\sqrt{2}}(2N_e - 2N_n) \approx \frac{5}{6}\sqrt{2} G_F N_e \quad \text{for Majorana neutrinos.} \tag{21}$$

The MSW resonance $\nu_{e_L} \to \nu_{\mu_L}$ occurs at a lower density where

$$\frac{\Delta m^2}{2E} cos2\theta = \sqrt{2} G_F N_e \tag{22}$$

for both neutrino types. The width of these two resonances are[37]

$$\delta N_e(\text{spin}) \sim N_e(\text{spin}) \frac{4E|\mu_{\mu e} B|}{\Delta m^2 cos2\theta},$$

$$\delta N_e(\text{MSW}) \sim N_e(\text{MSW}) tan2\theta, \tag{23}$$

where N_e(spin) and N_e(MSW) are the densities at which the two resonances occur.

In order for the depleted solar neutrino flux to exhibit an anti-correlation with the solar sunspot activity, the spin resonance has to occur in the convective zone. This requires $N_e(\text{spin}) \lesssim 0.2 N_A$. From Eq. (21), we obtain

$$\Delta m^2 cos2\theta \lesssim 2.9(3.2) \times 10^{-7} (\frac{E}{10\text{MeV}}) \text{eV}^2. \tag{24}$$

for Majorana (Dirac) neutrinos.

If the two resonance regions are well separated, i.e., they decouple, by satisfying

$$\delta N_e(\text{spin}) + \delta N_e(\text{MSW}) < N_e(\text{spin}) - N_e(\text{MSW}), \tag{25}$$

The transition probability at each resonance is[35]

$$P(\text{spin}) = \exp\Big[-\frac{4\pi E_\nu |\mu_{\mu e}|^2 B^2}{\Delta m^2 cos^2\theta |d(\ln N_e)/dr|_{res}}\Big],$$

$$P(\text{MSW}) = \exp\Big[\frac{-\pi \Delta m^2 sin^2 2\theta}{4E cos2\theta |d(\ln N_e)/dr|_{res}}\Big]. \tag{26}$$

The parameter space that satisfies the decoupling condition is

$$tan2\theta < 0.09(0.2) \text{ and } \Delta m^2 cos2\theta > 1.4(2) \times 10^{-7} (\frac{E}{10\text{MeV}}) \text{eV}^2 \tag{27}$$

for Majorana (Dirac) neutrinos. In this region, a substantial variation of the solar neutrino flux due to the solar magnetic field requires P(spin) to be sufficiently small. The conservative criterion is

$$P(\text{spin}) < 0.9, \tag{28}$$

which gives

$$\Delta m^2 cos^2\theta < 1.4(0.7) \times 10^{-7} (\frac{E}{10MeV}) \text{eV}^2. \tag{29}$$

An electron density profile $N_e/N_A = 245 \exp(-10.54 r/R_\odot) \text{cm}^{-3}$ is assumed, where N_A is the Avogadro's number and r is the distance to the center of the Sun.[7] The contradiction between Eq. (27) and Eq. (29) and Eq. (24) shows that the region of $\Delta m^2 cos2\theta \gtrsim$ few $\times 10^{-7} \text{eV}^2$ doesn't exhibit appreciable variation over the solar cycle.

At the region where the two resonance regions overlap, analytic techniques break down and a numerical simulation is necessary. But before we go into the detail and the result of the simulation, let us first discuss the effect of a possible megagauss or stronger magnetic field in the solar radiative zone. This strong field will deplete the neutrino fluxes as well as destroy their coherence. A megagauss field will have a

$$|\mu B| \sim 1 \times 10^{-14}\text{eV}. \tag{30}$$

The oscillation length between ν_{e_L} and other neutrinos is

$$l_{osc} \leq \frac{\pi \hbar c}{|\mu B|} \sim 5 \times 10^7\text{m} \ll 0.7R_\odot = 5 \times 10^8\text{m}. \tag{31}$$

Therefore the solar neutrino fluxes lose their coherence and are depleted more than they would if a weaker or no field exists in the radiative interior. The variation of the flux due to the variation of the magnetic field in the outer convective zone will then be less than the case when a weak field or no field is present in the solar radiative interior.

Hence we need only do numerical calculations for the case where no field exists in the solar radiative zone, to achieve a larger variation over the solar cycle. Fig. 1 (a) and (b) shows the 2.7 SNU contour of the chlorine experiment when the solar convective magnetic field is fully turned on, and the iso-R contours, for Majorana neutrinos (1(a)) and Dirac neutrinos (1(b)) that satisfies Eq. (10). (In the Dirac neutrino case, we assume $\mu_{e\mu}B = \mu_{\mu e}B = 4 \times 10^{-16}$eV and $\mu_{ee} = \mu_{\mu\mu} = 0$. If μ_{ee} or $\mu_{\mu\mu} > 0$, $\mu_{e\mu}$ and $\mu_{\mu e}$ will decrease accordingly, which will diminish the resonant effect, and cause a smaller variation over the solar cycle.) The smallest ratio that can be given is ~ 0.7 in case (a), and ~ 0.75 in case (b). No region on the parameter space satisfies Eq. (12). Therefore a neutrino magnetic moment and a solar convective field that satisfies Eq. (10) fails to yield the purported variation over the solar cycle in the Homestake experiment.

In the case of field ropes in the convective zone, the range of the field will be too short to induce any significant resonant effect. A strong field rope at the bottom of the convective zone may have a strength of 10^5 Gauss and a typical size of $\sim 10^3$ km. From Eq. (24), neutrinos with $\Delta m^2 cos2\theta \sim 10^{-7}(E/10\text{MeV})$ eV^2 will have a spin resonance between left and right components at the bottom of the convective zone. While from Eq. (26), the transition probabililty is about 0.5, the transition region has a size of (from Eq. (23))

$$\delta N_e(\text{spin})|dr/dN_e| \sim |dr/d(lnN_e)|\frac{4E|\mu_{\mu e}B|}{\Delta m^2 cos2\theta} \sim 4 \times 10^4\text{km}, \tag{32}$$

which is much larger than the size of the field rope. In other words, the resonant transition is far from complete. Therefore the presence of strong field ropes doesn't affect our previous conclusion in any significant sence.

If we further relax the bound on μB from Eq. (10) by doubling the right-hand side,

$$|\mu B| \leq 2(1.4) \times 10^{-7} \mu_B \cdot \text{Gauss}, \tag{33}$$

Fig. 2 (a) and (b) show that regions that yield large depletions and variations exist for both Majorana and Dirac neutrinos. For Majorana neutrinos, this region is $\Delta m^2 < 10^{-7}\text{eV}^2$. For Dirac neutrinos, two possible regions exist: the region that is similar to the Majorana case, $\Delta m^2 < 10^{-7}\text{eV}^2$; and the large mixing angle region. The minimal variation can be as low as 0.2 for the Majorana neutrinos and 0.5 for the Dirac neutrinos.

If we only use the bound on the convective field from the ^{7}Li consideration, solutions that satisfy Eq. (12) also exist for both Majorana and Dirac cases. Fig. 3 (a) and (b) shows the same graph as Fig. 1 but with μB satisfying Eq. (11) and no field in the radiative zone, for Majorana neutrinos and Dirac neutrinos. Again, for Majorana neutrinos, a possible solution with $\Delta m^2 \lesssim 10^{-7}$ eV^2 exists; for Dirac neutrinos, beside the region $\Delta m^2 \lesssim 10^{-7}$ eV^2, the large angle region is also possible.

Our calculation in Fig. 1–2 differs from the calculation of Balantekin *et al.* [38] in: (1) we have used the published and well-justified stricter bounds on both the neutrino magnetic moment and the solar magnetic field in the convective zone; (2) we assume a uniform distribution of the field, instead of the Woods-Saxon shape or the configuration suggested by Sofia *et al.*, both of which are adopted by Balantekin *et al.*, due to our conservative assertion that the interior configuration of the field is very complex and unknown. A uniform distribution will yield a larger time variation over the solar cycle, when the upper limit on the field is fixed. Therefore our limit is more conservative. We have also discussed the effect of a possible strong magnetic field in the solar radiative interior, which will diminish the variation. Our calculation for zero field in the radiative zone can serve as an upper limit on reality because: (1) we relax the bound on μB from Eq. (9) to Eq. (10) in our calculation; (2) we assume a uniform field configuration in the convective zone, while the actual field is weaker at the surface than at the bottom; (3) a strong magnetic field in the radiative zone will weaken the variation over the solar cycle.

Conclusion

By reviewing and using the current constraints on the neutrino magnetic moments and on the solar magnetic field, Eq. (10), we have calculated the depletion rate of the neutrino flux and the variation over the solar cycle on the neutrino mixing parameter space. With these constraints, no solutions can be found to yield an observable anti-correlation between the neutrino flux and the sunspot activity in the chlorine experiment, for both Dirac neutrinos and Majorana neutrinos. However such solutions may be found if we further relax the bounds to Eq. (33) or Eq. (11), but such relaxation is unjustified at this time. We therefore conclude that if there is ever shown to be statistically significant anti-correlation between the solar neutrino flux and the solar cycle, such anti-correlation cannot be easily explained by neutrino magnetic moment effects, the only proposed physical explanation to date (see discussion in appendix on statistics). This may leave the unattractive alternative that if such solar neutrino variations exist, they are instead created by some as yet unknown systematic effects in the experiment itself. The key here would be whether or not similar effects are observed in other solar neutrino experiments. If not, then the chlorine experiment may be called into question to the degree that such variations are observed.

Acknowledgement:

We thank E. N. Parker, D. Q. Lamb, T. J. Loredo and L. Tao for valuable discussions. This work is supported by the NSF, the DoE (nuclear) and NASA at the University of Chicago, by the DoE at Livermore, and by the DoE and by NASA through grant 2381 at Fermilab.

Appendix

On the Statistical study of the Anti-correlation Between the ^{37}Cl Capture Rates and the Sunspot Numbers

The statistical significance of the claimed anti-correlation has been extensively investigated.[39,40,41] The concensus seems to be that though the anti-correlation cannot be ruled out, it is also not statistically established. Furthermore, the Kamiokande II data didn't show any significant variation during the period 1987–1990 when there was a major change in sunspot numbers, which provided evidence against the correlation in the Homestake experiment.[4] On the other hand, most statistical analyses done to date do indicate a non-negligible probability that the data could be from a constant counting rate.[39,40,41]

Two hypotheses have been tested to explore the purported anti-correlation: (1) a constant capture rate (null hypothesis); (2) a correlation between the neutrino capture rate r and the sunspot number $N_{sunspot}$

$$r = a + b \times N_{sunspot}, \tag{A-1}$$

where a and b are two constants. When $b = 0$, hypothesis (2) is reduced to hypothesis (1).

Bahcall *et al.* did a χ^2 test to the 1970–84 data to evaluate the statistic significance of the two hypotheses. Since the neutrino capture rates cannot be less than zero, the data of some runs have asymmetric errors. When the upper errors are used to represent the errors of the data, Bahcall *et al.* found that hypothesis (1) had a P value (as defined to be the probability of that a random set of data would yield a larger χ^2 than the tested data;[42] a hypothesis that has a P of 0.05 is ruled out at 95% C. L..) of 61%, while hypothesis (2) had a P of 75%. When average errors (averaging over the upper and the lower errors arithmatically) are adopted, the two hypotheses have P's of only 2% and 9% respectively. Furthermore, they found that the significance of hypothesis (2) was very sensitive to the four low counting runs around 1980. When the four runs were removed, the best fit to the data was practically constant.

Other statistical tests have also been done. For example, Bieber et *al.* applied F test to the data to evaluate the improvement in probability of hypothesis (2) over hypothesis (1). They concluded that b is non-zero at 99.6% C. L.[41]

However, due to the low counting nature ($\sim$ 10 counts for each run) and the small signal to noise ratio of the Homestake experiment, the conventional gaussian statistical techniques are known to fail and hence most tests done to date may not seem adequate. They are sensitive to the errors quoted in the experiment, which themselves are not well understood. A maximal likelihood procedure is more adequate to analyze the data. A systematic investigation would require to calculate the likelihood of each individual neutrino event assuming certain correlating hypotheses and Poisson distribution, and maximize the product of such likelihoods over the entire data set.[43] So far such an investigation hasn't been done.

Filippone and Vogel have applied the maximal likelihood procedure to each individual run (which has $\sim$ 10 neutrino events over the period of $\sim$ 50 days).[40] They concluded that when upper errors were used, the null hypothesis has a P of 1.8% and the second hypothesis has a P of 5.7%. They further found that an 11-year periodic fit to the data had a P of less than 5%, while the best periodic fit was with a period of 4.7 years and a P of 8.3%.

The neutrino magnetic moment scenario is so far the only physical solution to explain the claimed anti-correlation solution.[10,35] In this scenario, the solar neutrino flux is directly related to the solar convective magnetic field on the routes of solar neutrinos, whose strength is roughly represented by the sunspot numbers at the solar surface. Therefore, the linearly sunspot-correlating hypothesis (2) is an obviously oversimplified representation of such correlation between the capture rates and the solar magnetic fields. On the one hand the correlation may not be linear; on the other hand, though the sunspot numbers reflect the strength of the solar convective magnetic fields in general, it by no means describes the detail of the fields the neutrinos have encountered with, due to the complexities of the solar magnetic fields (for example, the opposite polarization on each side of the solar equator implies that the field is rather weak near the equator even in solar active years).[22] Therefore in this appendix, we attempt to explore the effect on the statistical significance of the two hypothesis by this second factor.

On the experimental side, one concern may be that how would hypothetical systematic errors in the experiment could affect the the claimed anti-correlation. It has been occasionally suggested that unanticipated systematic uncertainties might exist in the Homestake experiment.[11] Morrison argued that inconsistent neutrino capture rates had been observed during the period 1970–1984 and thereafter. The averaged neutrino capture rate during 1970–1984 is 2.1 $\pm$0.3 SNU.[44] Then there were two pump failures during 1984–1985. After new pumps were installed and the experiment was resumed, the averaged rate for the period 1986–1988 (run 90–100) is 3.6$\pm$0.7 SNU.[7] (However, it is to be noted that various tests have been done on the Homestake experiment and no source of unanticipated systematic errors has ever been found.[7] Pump replacements prior to 1984 also indicated no sign of affecting the counting rates. Up to Run 109, the unweighted average rates are 2.0 ± 0.3 SNU and 2.8 ± 0.6 SNU for data before and after the pump failures, which show no significant discrepancy.[45] The average rate from the maximal likelihood calculation for data after 1984 is not available.) If any unexpected systematic error does or did exist, the conclusion on the claimed correlation may be seriously affected. We will attempt to explore the effect of hypothetical systematic errors quantitatively later in this appendix.

One way to incorporate the uncertainty in sunspot numbers in the problem is to assume that the sunspot number represents the mean field strength, and the local field that plays a role in depleting the solar neutrinos satisfies a Gaussion distrubution. Therefore when applying the χ^2 test of Bahcall *et al.* to the Homestake data, one needs to consider not only the experimental errors, but also the errors of sunspot numbers in representing the true acting fields, which we assume to have a standard deviation of 30% of the sunspot numbers (mean field stength). The new χ^2 test is then minimizing

$$\chi^2 = \sum_{Run\ i} \left\{ \frac{r_i - [a + b \times N_{sunspot,i}]}{\sqrt{\sigma^2_{exp,i} + b^2 \times dN^2_{sunspot,i}}} \right\}^2, \tag{A–2}$$

in which $dN_{sunspot,i}$ is the error in sunspot numbers and $dN_{sunspot,i} = 0.3N_{sunspot,i}$. Apparently if $b \equiv 0$, the equation yields the same results as in Bahcall's test where $dN_{sunspot,i} = 0$. But if $b \neq 0$, Eq. (A–2) yields a smaller χ^2 than in Bahcall's test. We have repeated the procedure of Bahcall et al. for the updated Homestake data of 1970–1990, assuming both $dN_{sunspot,i} = 0$ and $dN_{sunspot,i} = 0.3N_{sunspot,i}$. The results are summarized in Table A–1.

We have also repeated the procedure of Filippone and Vogel to the Homestake data. The original test is to maximize

$$\mathcal{L} = \prod_{Run\ i} P_i = \prod_i \frac{\mu_i^{n_i} \exp(-\mu_i)}{n_i!}, \tag{A–3}$$

where μ_i and n_i are the expected number of counts and the real number of counts. They are effectively obtained from the counting rate r_i and its error dr_i by assuming the Poisson distribution to each run:

$$n_i = (r_i/dr_i)^2, \quad \mu_i = n_i(\bar{p}/r_i), \tag{A–4}$$

where $\bar{p}$ is the expected capture rate that we attempt to fit the data. Equation $\bar{p} = a + b \times N_{sunspot}$ is assumed to represent the two hypotheses by letting $b \equiv 0$ or $b \neq 0$. The statistical significance is represented by the quantity $-2ln\lambda = -2ln[\mathcal{L}(\bar{p})/\mathcal{L}(q)]$, where $\mathcal{L}(\bar{p})$ is the likelihood function when a hypothesis $\bar{p}$ is fitted, and $\mathcal{L}(q)$ is the likelihood function when the real data are fitted. When the number of data points is large, as in our case, the quantity $-2ln\lambda$ distributes like a χ^2 distribution.

In order to incorporate the uncertainty in the sunspot number in the test, we assume $p = a + b \times (N_{sunspot} + dN_{sunspot})$, where $dN_{sunspot}$ satisfies a Gaussian distribution with a mean of 0 and a standard deviation of $0.3N_{sunspot}$. By Monte Carlo simulating the runs, one gets a good estimate of the goodness of each fit. Table A–2 lists our results before and after considering the sunspot uncertainty. The likelihood after considering the sunspot uncertainty is obtained from the 100 Monte Carlo simulation.

From the table A–1 and A–2 we can see that even with an assumed 1σ sunspot relative uncertainty of 30%, the goodness-of-fit of each hypothesis is not dramatically improved. When doing the χ^2 test with upper experimental errors, the realistic experimental errors are apparently overestimated. Therefore the large P of 40–50% in this case doesn't have much physical meaning, as can be seen from the extremely small P value when average experimental errors are used. Overall, neither hypotheses shows great statistical significance. In particular, the constant rate hypothesis can still be marginally ruled out at 98% C. L. But the conventional wisdom is that 98% C. L. isn't strong enough to rule out a hypothsis under circumstances where the statistics is low.

Compared with the χ^2 test results of Bahcall *et al.*, The P value of each hypothesis is smaller for 1970–1990 data than that for 1970–1984 data as calculated by Bahcall *et al.*. This is due to the difference in the averaged capture rates before and after the pump failures in 1984–1985. By using the test of Filippone and Vogel, we found that for the total 87 runs (1970–1990), the first 66 runs (1970–1984) yield an average rate of 0.51 ± 0.04 event/day, while the last 19 runs (1986–1990) yield an average of 0.68 ± 0.08 event/day. Supposely if there did exist unanticipated systematic errors that caused the difference, the outcome of above tests could be very different. Therefore we introduce by hand a Poisson distributed systematic offset to the 1970–84 data, with the average offset to be 0.17 event/day that is the right amount needed to equilize the two average rates before and after the pump failures, and repeat the test of Filippone and Vogel. To make its effect prominent, we neglect the uncertainty in sunspot numbers. We find a sharp decrease in $-2ln\lambda$ for both hypotheses. The P for $a \sim 0.7$ event/day and $b \sim 10^{-3}$ event/day/sunspot easily exceeds 0.5. The null hypothesis has a maximal P of ~ 0.6 at $a \sim 0.67$ event/day.

In summary, the consideration of the uncertainties in sunspot numbers doesn't introduce considerable improvement of the statitistical significance of either the constant rate hypothesis or the sunspot-correlating hypothesis. In particular, one may still argue that the constant rate hypothesis is ruled out, though with low confidence. However, hypothetical systematic offset of part of the data may change their statistical significance dramatically.

Since the chlorine experiment sees mostly ^8B neutrinos plus some low energy ^7Be, CNO and *pep* neutrinos, and the Kamiokande II experiment sees only high energy ^8B neutrinos (> 8 MeV), the fact that the Kamiokande II experiment didn't observe any appreciable event rate variation during 1987–1989 (when there is a major change in sunspot numbers) serves as an counter proof to the possible correlation in the chlorine experiment. However, the 3-year operation of the Kamiokande II experiment only rules out the constant rate hypothesis at 80%–90% C. L., depending on the energy threshold cut.[46] Therefore one cannot draw any statistically significant conclusion with regard to the time variation of the solar neutrino flux based on current experimental data.

One cannot attribute the variation in the chlorine experiment to the low energy neutrinos that the Kamiokande II doesn't see. Because this requires the low energy neutrinos not being significantly depleted when the solar convective magnetic field is weak, while the high energy ^{8}B neutrinos being severely depleted to meet the observed deficit. This requirement can only be realized in the MSW matter mixing when $10^{-5}\mathrm{eV}^2 < \Delta m^2 < 10^{-4}\mathrm{eV}^2$, among a wide range of solutions.[47] But neutrino mixing in this parameter range cannot be depleted significantly by the solar magnetic field in the convective zone as shown in our calculation in the text. Even if the above reconcilation between the two experiments is valid, it implies that the gallium experiments which observe mostly low energy neutrinos should see a much more amplified variation over the solar cycle than the Homestake experiment did, which remains to be seen in the near future.

An argument based on OVV mechanism is made that the extra electromagnetic current scattering between the neutrinos and the electrons due to neutrino magnetic moments could obscure the variation of the weak current events. However, the astrophysical limits on the neutrino magnetic moments have limitted the electromagnetic current events to be much smaller than the weak events, thus invalidated the argument. According to Bethe, the cross section of the neutrino electron scattering due to the neutrino magnetic moment μ_ν is[48]

$$\sigma_{EM} = \pi(e/\hbar c)^2 \mu_\nu^2 ln(q_{max}/q_{min}), \tag{A-6}$$

where q_{max} and q_{min} are the maximal and minimal transfered momentum. For relativstic scattering, $ln(q_{max}/q_{min}) \sim \mathcal{O}(1)$, taking $\mu_\nu < 10^{-11}\mu_B$,

$$\sigma_{EM} \sim \pi(e/\hbar c)^2 \mu_\nu^2 < 10^{-46}\mathrm{cm}^2 \ll \sigma_W \approx 10^{-44}\mathrm{cm}^2. \tag{A-7}$$

Therefore if the Kamiokande experiment does see constant fluxes and the Homestake experiment does see fluxes correlating with sunspot numbers, the conflict between the two experiments seems irreconcilable. The three-year operation of the Kamiokande II experiment may not appear long enough to reveal any (or no) correlation over 11-year sunspot cycle. More data from future operation of these solar neutrino experiments (especially GALLEX and SAGE) are definitely needed to resolve the issue.

Reference:

1. J. K. Rowley, B. T. Cleveland, R. Davis, Jr., in *Proc. XIII Int. Conf. Neutrino Phys. and Astrophys.* (NEUTRINO'88), eds. J. Schneps *et al.* (World Scientific, Singapore, 1989), p. 518.

2. John N. Bahcall and Roger K. Ulrich, *Rev. Mod. Phys.* **60**, 297 (1988).

3. S. Turck-Chièze, S. Cahn, M. Cassé, and C. Doom, *Ap. J.*, **335**, 415 (1988). It is pointed out by Bahcall that their model overestimated the collective effects on the photon-electron scattering opacity. After a correction is made, their prediction for the ^{37}Cl rate increases from the original 5.8 SNU to about 6.4 SNU, with the increase mainly in ^{8}B neutrinos. Please refer to J. N. Bahcall and M. H. Pinsonneault, to be published in *Rev. Mod. Phys.* (1992).

4. K. S. Hirata *et al.*, *Phys. Rev. Lett.* **65**, 1297 (1990).

5. V. N. Gavrin, talk at the *26th Intl. Conf. on High Energy Physics*, Dallas, 1992.

6. P. Anselmann, *et al.*, 1992, *Phys. Lett.* B (in press).

7. John N. Bahcall, *Neutrino Astrophysics*, Cambridge University Press (1989).

8. L. Wolfenstein, *Phys. Rev.* D **17**, 2369 (1978); S. P. Mikheyev and A. Yu. Smirnov, *Sov. J. Nucl. Phys.* **42**, 913 (1985).

9. R. Davis, Jr., in *Proc. of 7th Workshop on Grand Unification, ICOBAN'86*, 1987, Toyama, Japan, ed. J. Arafune (World Scientific) p.237.

10. L. B. Okun, M. B. Voloshin, and M. I. Vysotsky, *Sov. J. Nucl. Phys.*, **44**, 440 (1986).

11. D. Morrison, *Particle World*, **Vol. 3**, No. 1, 30 (1992).

12. B. W. Lee and R. E. Shrock, *Phys. Rev.* D **16**, 1444 (1977).

13. M. Fukugita and T. Yanagida, *Phys. Rev. Lett.* **58**, 1807 (1987); K. S. Bacu and V. S. Mathur, *Phys. Lett.* B **196**, 218 (1987); J. E. Kim, *Phys. Rev.* D **14**, 3000 (1986).

14. W. J. Marciano and Z. Parsa, *Annu. Rev. Nucl. Phys. Part. Sci.*, **36**, 171 (1986).

15. P. Sutherland *et al.*, *Phys. Rev.* D **13**, 2700 (1976).

16. J. Morgan, *Phys. Lett.*, B **102**, 247 (1981).

17. D. N. Schramm and J. W. Truran, *Physics Report*, **189**, No. 2, 89 (1990).

18. R. Barbieri and R. Mohapatra, *Phys. Rev. Lett.* **61**, 27 (1988); J. M. Lattimer and J. Cooperstein, *Phys. Rev. Lett.* **61**, 23 (1988).

19. D. Nötaold, *Phys. Rev.* D **38**, 1658 (1988).

20. M. B. Voloshin, *JETP Lett.*, **47**, 501 (1988).

21. Georg G. Raffelt, *Phys. Rev. Lett.* **64**, 2856 (1990).

22. For a review on the solar magnetic activity, see E. N. Parker, *Cosmical Magnetic Fields*, (Clarendon Press, Oxford, 1979) Ch. 1 and Ch. 21, and reference therein.

23. R. Rosner and N. O. Weiss, *Ap. J.*, 1992, in press.

24. S. J. Vainshtein, E. N. Parker and R. Rosner, *Ap. J.*, 1992, in press.

25. Ref. 22, pp. 147–151.

26. D. J. Galloway and N. O. Weiss, *Ap. J.*, **243**, 945 (1981).

27. J. H. M. M. Schmitt, R. Rosner and U. Bohn, *Ap. J.*, **282**, 316 (1984).

28. J. Schmitt and R. Rosner, *Ap. J.*, **265**, 901 (1983).

29. A. Maeder, *Astr. Ap.*, **40**, 303 (1975).

30. S. J. Vainshstein and R. Rosner, *Ap. J.*, **376**, 199 (1991); F. Cattaneo and S. J. Vainshtein, *Ap. J.*, **376**, L21 (1991); S. J. Vainshtein and F. Cattaneo, *Ap. J.*, **393**, 165 (1992).

31. E. N. Parker, *Ap. J.*, **286**, 666 (1984).

32. E. A. Müller *et al.*, *Solar Phys.*, **41**, 53 (1975).

33. Terry Walker *et al.*, *Ap. J.* **376**, 51 (1991).

34. E. Parker, private communication.

35. C.-S. Lim and W. J. Marciano, *Phys. Rev.* D **37**, 1368 (1988).

36. Calculated from Table 4.5, ref. 7.

37. H. Minakata and H. Nunokawa, *Phys. Rev. Lett.* **63**, 121 (1989).

38. A. B. Balantekin, *et al.*, *Phys. Rev.* D **41**, 3583 (1990).

39. J. N. Bahcall, G. B. Field and W. H. Press, *Ap. J.*, **320**, L69 (1987).

40. B. W. Filippone, P. Vogel, *Phys. Lett.* B, **246**, 546 (1990).

41. J. W. Bieber *et al.*, *Nature*, **V 348**, 407 (1990).

42. P. R. Bevington, *Data Reduction and Error Analysis for the Physical Science*, McGraw-Hill, 1969.

43. D. Q. Lamb, priv. comm.

44. J. K. Rowley, B. T. Cleveland and R. Davis, Jr., in *Solar Neutrinos and Neutrino Astronomy*, eds. M. L. Cherry, K. Lande and W. A. Fowler, AIP conf. Proc. No. 126, AIP, New York, 1984, p. 1.

45. Calculated from K. Lande, K. Lande, *25th Intl. Conf. on High Energy Physics*, eds. K. K. Phua and Y. Yamaguchi, **Vol. 1**, 667 (1990).

46. Ken-ichi Kihara, ICRR-Report-274-92-12.

47. Different solutions generate different neutrino spectrums. For example, the diagonal part of the MSW solution has a higher depletion rate at lower energy; the vertical part of the MSW solution has a uniform depletion over the energy spectrum; The vaccum oscillation will deplete the low energy neutrino by half; The original OVV solution deplete the solar neutrino uniformly. For a review, see Ch 9 of ref. 7. and references therein.

48. H. Bethe, *Proc. Camb. Phil. Soc.*, **31**, 108 (1935).

Figure caption:

Fig. 1 Assuming $|\mu B| = 1(0.7) \times 10^{-7}\mu_B \cdot$ Gauss, for the Majorana (Dirac) transitional magnetic moment, The solid line is the 2.7 SNU contour for the chlorine experiment when the field is on; the long-dashed line is the 2.7 SNU contour for the chlorine experiment when the field is off; the short-dashed line is the iso-variation contours for the chlorine experiment. (a) Majorana neutrinos, (b) Dirac neutrinos. No field is present in the radiative zone.

Fig. 2 The same graph as Fig. 1 but assuming $|\mu B| = 2(1.4) \times 10^{-7}\mu_B \cdot$ Gauss, for the Majorana (Dirac) transitional magnetic moment.

Fig. 3 The same graph as Fig. 1 but assuming $B = 4 \times 10^5$ Gauss and extends 3×10^4 km at the bottom of the convective zone, $B = 1000$ Gauss for the rest of the convective zone, and $\mu = 3(2) \times 10^{-12}\mu_B$ for the Majorana (Dirac) transitional magnetic moment.

TABLE A–1 χ^2 test of Bahcall *et al.* to the two hypotheses

Hypothesis	parameter	Eq. (2)		Eq. (3) with $dN_{sunspot} = 0.3N_{sunspot}$	
		Upper Error	Average Error	Upper Error	Average Error
$b \equiv 0$	a (event/day)	0.40	0.29	0.40	0.29
	P	18%	10^{-4}	18%	10^{-4}
$b \neq 0$	a (event/day)	0.54	0.45	0.59	0.50
	b (event/day/sunspot)	−0.0016	−0.0017	−0.0021	−0.0020
	P	40%	2×10^{-3}	50%	1%

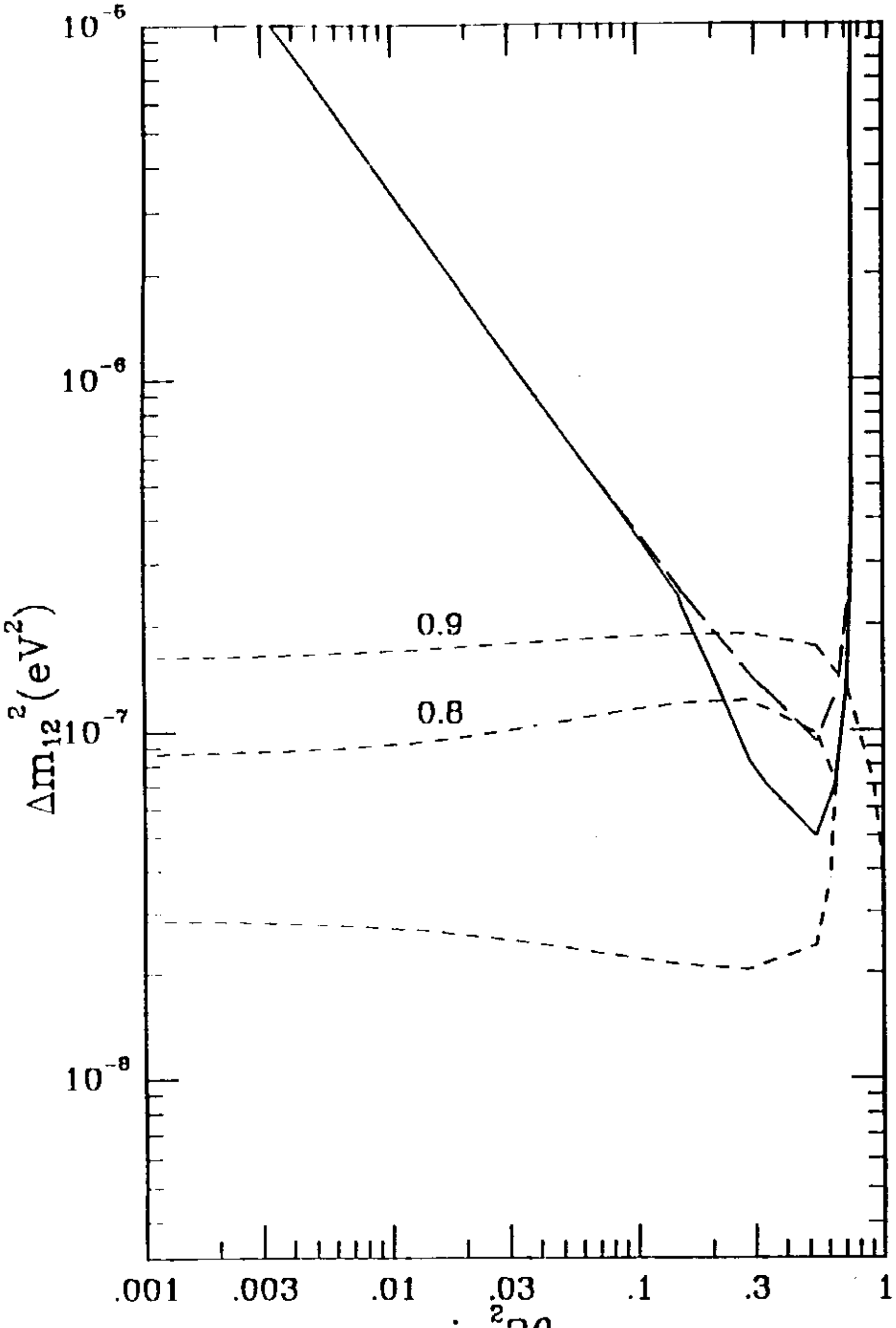

$\Delta m_{12}^2 (eV^2)$
10^{-5}
10^{-6}
10^{-7}
10^{-8}
0.9
0.8
.001
.003
.01
.03
.1
.3
1
$\sin^2 2\theta$

Fig. 1(a)

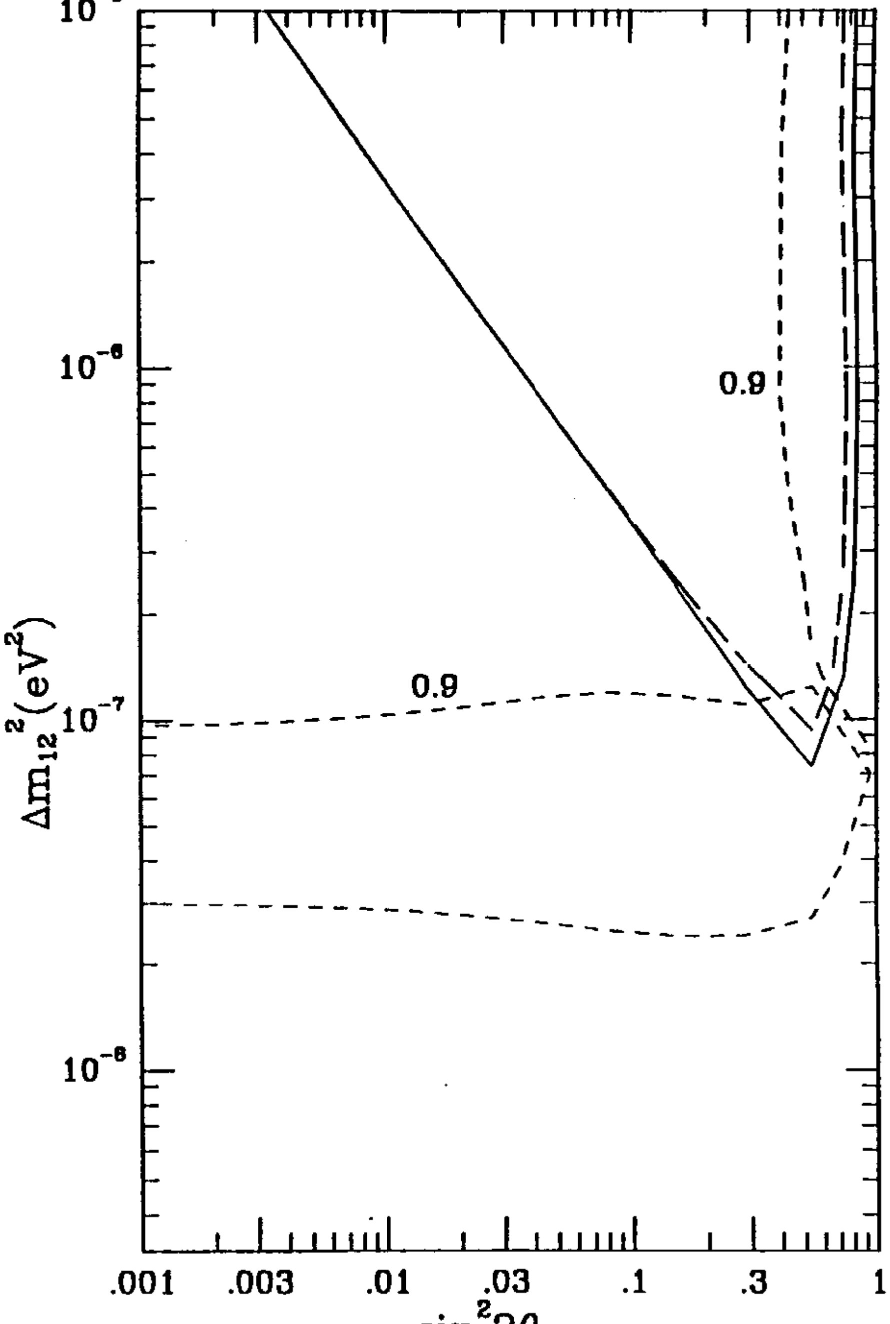

$\Delta m_{12}^2 (eV^2)$
10^{-5}
10^{-6}
10^{-7}
10^{-8}
0.9
0.9
.001
.003
.01
.03
.1
.3
1
$\sin^2 2\theta$

Fig. 1(b)

TABLE A–2 Test of Filippone and Vogel to the two hypotheses

Hypothesis	Parameter	W/O sunspot uncertainty	W/ 30% sunspot uncertainty
$b \equiv 0$	a (event/day)	0.556±0.034	0.56±0.035
	P	2%	2%
$b \neq 0$	a (event/day)	0.63±0.035	$\sim$ 0.65
	b (event/day/sunspot)	−0.001±0.0003	$\sim$ 0.0015
	P	2.5%	5%

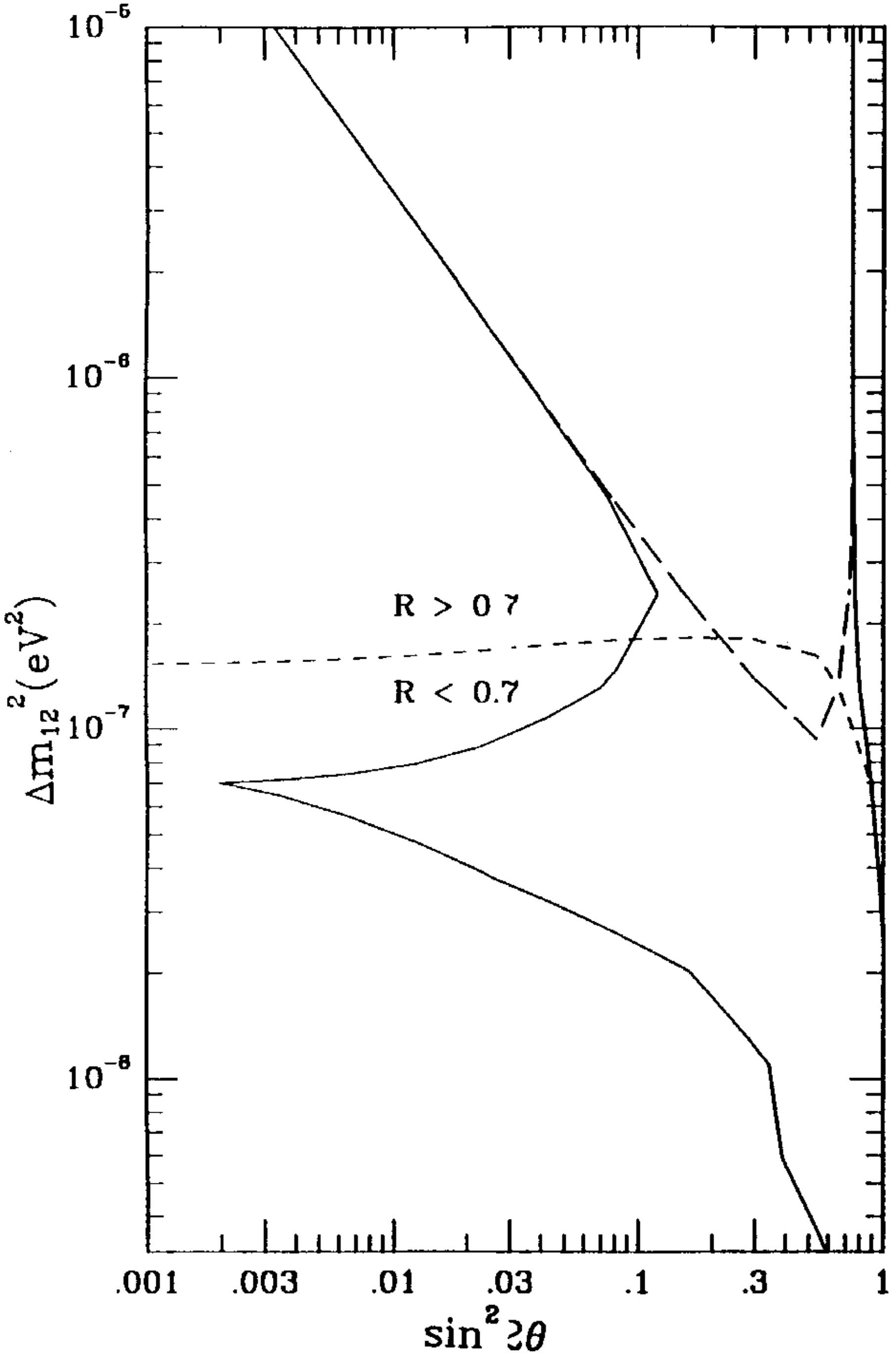

$\Delta m_{12}^2(eV^2)$
10^{-5}
10^{-6}
10^{-7}
10^{-8}
R > 0 7
R < 0.7
.001
.003
.01
.03
.1
.3
1
$\sin^2 2\theta$

Fig. 2(a)

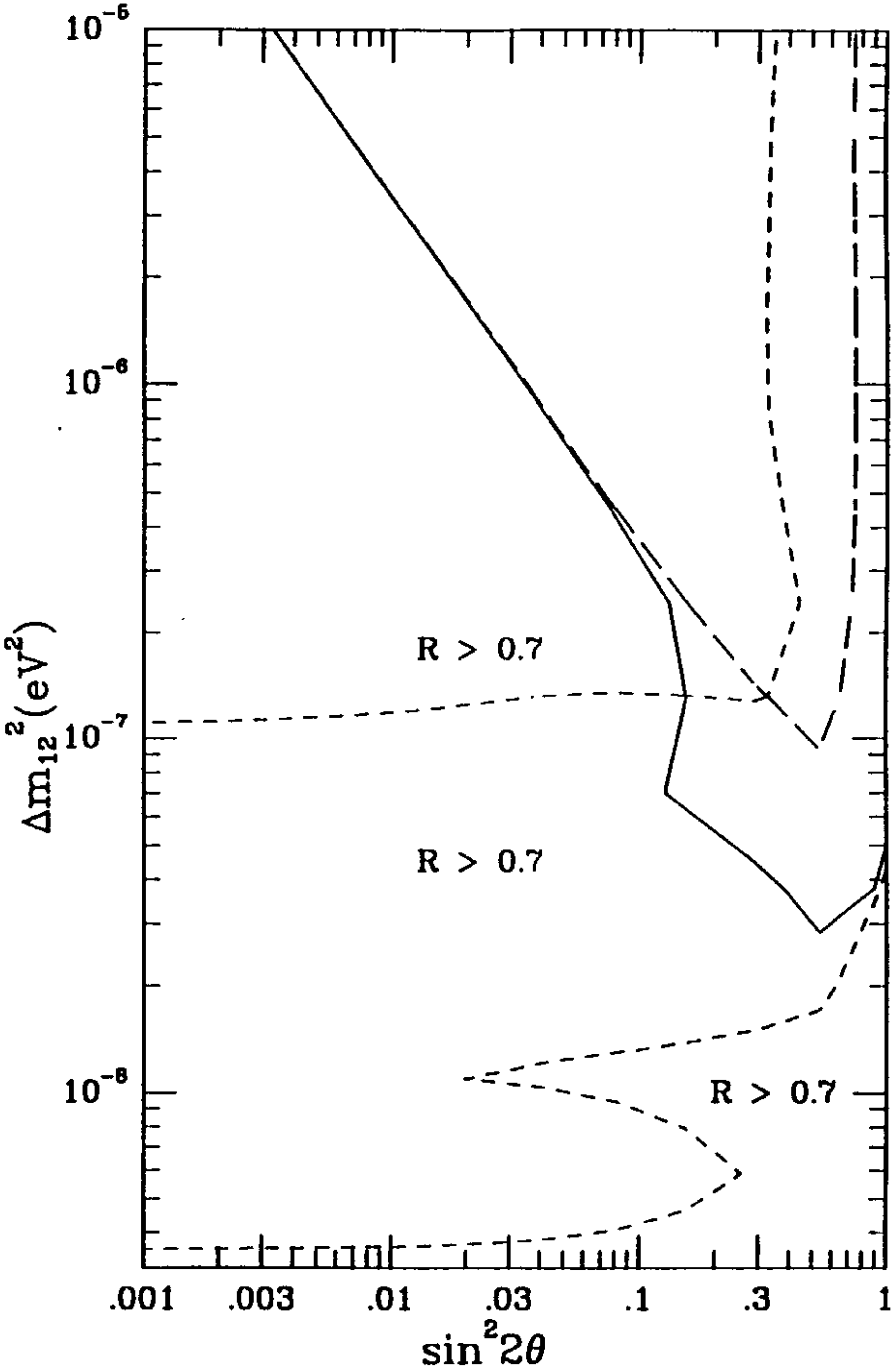

$\Delta m_{12}^2(eV^2)$
10^{-5}
10^{-6}
10^{-7}
10^{-8}
R > 0.7
R > 0.7
R > 0.7
.001
.003
.01
.03
.1
.3
1
$\sin^2 2\theta$

Fig. 2(b)

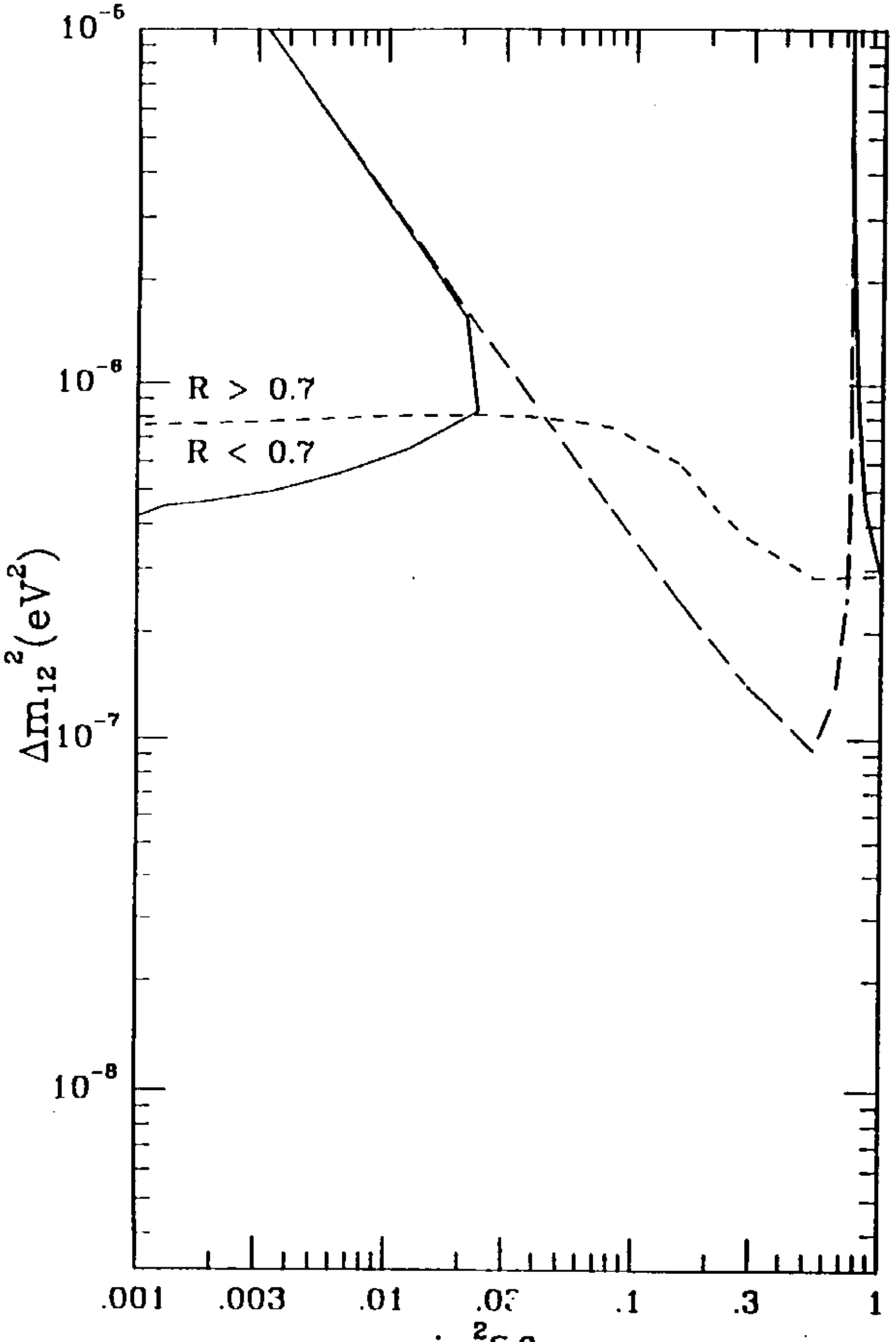

$\Delta m_{12}^2 (eV^2)$
10^{-5}
10^{-6}
10^{-7}
10^{-8}
R > 0.7
R < 0.7
.001
.003
.01
.03
.1
.3
1
$\sin^2 2\theta$

Fig. 3(a)

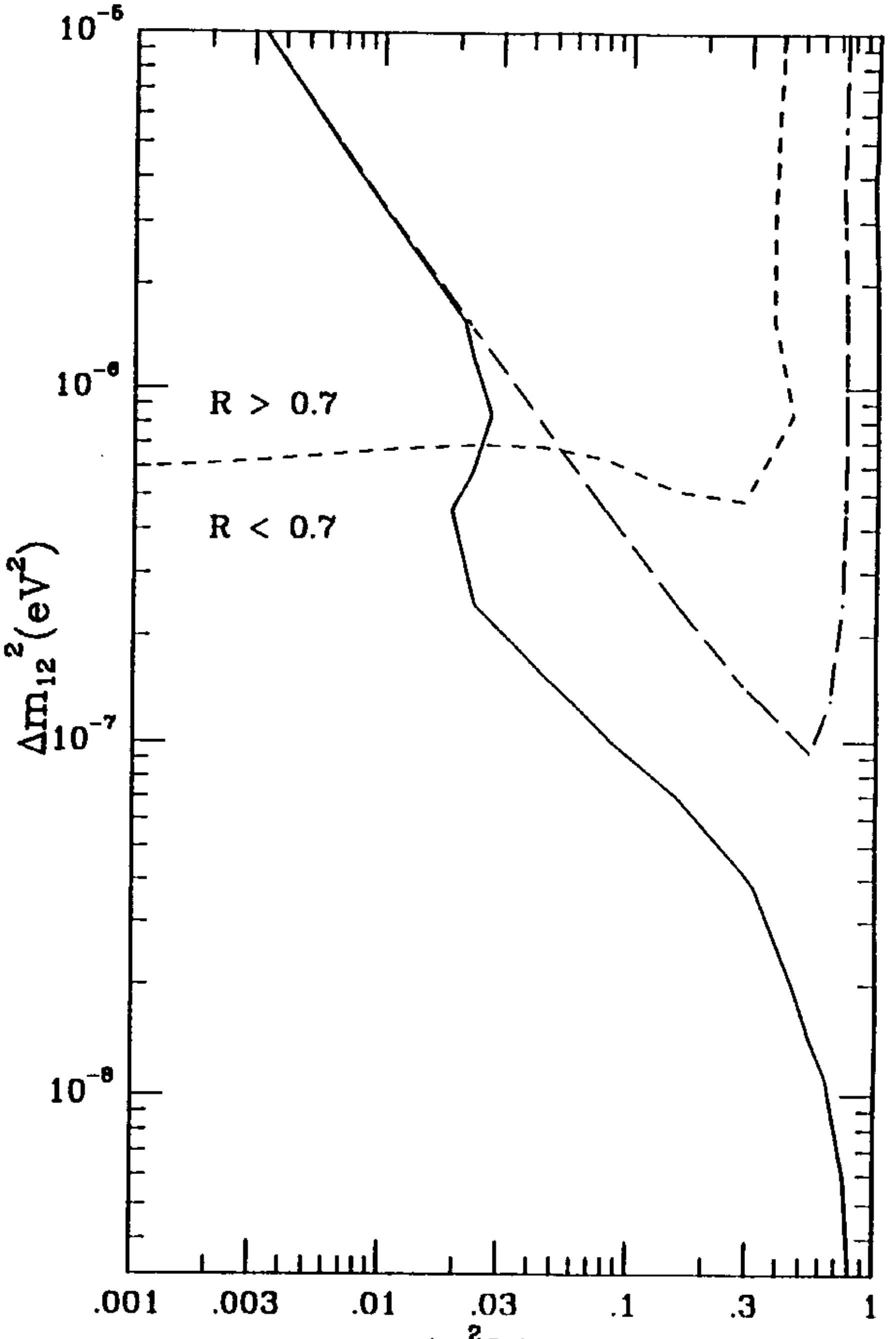

$\Delta m_{12}^2 (eV^2)$
10^{-5}
10^{-6}
10^{-7}
10^{-8}
R > 0.7
R < 0.7
.001
.003
.01
.03
.1
.3
1
$\sin^2 2\theta$

Fig. 3(b)